

sition of ASW can also occur when a particle or body is passing through a water cloud with a large relative velocity. In other cases, such as the formation of comets (1), porous ASW may result when omnidirectional deposition of the water molecules occurs.

Adsorption, diffusion, reaction, and desorption of volatile gases on and through ASW are expected to depend critically on the morphology. These elementary kinetic processes form the microscopic basis for a variety of important astrophysical phenomena such as the outgassing of comets (19, 20, 30, 31) and chemical reactions in interstellar clouds (3). Our results show that, for porous ASW, large quantities of gases can adsorb at temperatures above the nominal equilibrium vapor pressure. The thermal conductivity of ASW, which is important in the thermal processing of icy bodies, should also depend sensitively on its morphology. The temperatures attained in the objects help to determine the extent of densification of the ASW and the diffusion, reaction, or desorption of gases trapped in the ASW. Examples of thermal processing include comets as they orbit the sun (30, 32) and particles in the rings of Saturn as they pass into and out of the planet's shadow (2).

References and Notes

1. P. Jenniskens and D. F. Blake, *Science* **265**, 753 (1994).
2. R. Smoluchowski, *ibid.* **201**, 809 (1978).
3. A. G. G. M. Tielens and L. J. Allamandola, in *Composition, Structure, and Chemistry of Interstellar Dust*, J. D. J. Hollenbach and H. A. Thronson, Eds. (Reidel, Dordrecht, Netherlands, 1986), pp. 397–469.
4. R. J. Speedy, P. G. Debenedetti, R. S. Smith, C. Huang, B. D. Kay, *J. Chem. Phys.* **105**, 240 (1996).
5. P. G. Debenedetti, *Metastable Liquids: Concepts and Principles* (Princeton Univ. Press, Princeton, NJ, 1996).
6. J. A. Ghormley, *J. Chem. Phys.* **46**, 1321 (1967).
7. E. Mayer and R. Pletzer, *Nature* **319**, 298 (1986).
8. R. Pletzer and E. Mayer, *J. Chem. Phys.* **90**, 5207 (1989).
9. A. W. Adamson, L. M. Dormant, M. Orem, *J. Colloid Interface Sci.* **25**, 206 (1967).
10. J. Ocampo and J. Klinger, *ibid.* **86**, 377 (1982).
11. M. T. Leu, L. F. Keyser, R. S. Timonen, *J. Phys. Chem. B* **101**, 6259 (1997).
12. A. H. Delsemme and A. Wenger, *Science* **167**, 44 (1970).
13. B. A. Seiber, B. E. Wood, A. M. Smith, P. R. Muller, *ibid.* **170**, 652 (1970).
14. J. A. Ghormley and C. J. Hochanadel, *ibid.* **171**, 62 (1971).
15. A. H. Narten, C. G. Venkatesh, S. A. Rice, *J. Chem. Phys.* **64**, 1106 (1976).
16. M. S. Westley, G. A. Baratta, R. A. Baragiola, *ibid.* **108**, 3321 (1998).
17. D. E. Brown *et al.*, *J. Phys. Chem.* **100**, 4988 (1996).
18. S. J. Gregg and K. S. W. Sing, *Adsorption, Surface Area, and Porosity* (Academic Press, London, ed. 2, 1982).
19. A. Bar-Nun, G. Herman, D. Laufer, *Icarus* **63**, 317 (1985).
20. A. Bar-Nun, J. Dror, E. Kochavi, D. Laufer, *Phys. Rev. B* **35**, 2427 (1987).
21. A. Bar-Nun, I. Kleinfeld, E. Kochavi, *ibid.* **38**, 7749 (1988).
22. K. P. Stevenson, G. A. Kimmel, Z. Dohnálek, R. S. Smith, B. D. Kay, data not shown.
23. E. Mayer and R. Pletzer, *J. Chem. Phys.* **80**, 2938 (1984).

24. A. Hallbrucker and E. Mayer, *J. Chem. Soc. Faraday Trans.* **86**, 3785 (1990).
25. A. L. Barabasi and H. E. Stanley, *Fractal Concepts in Surface Growth* (Cambridge Univ. Press, Cambridge, 1995).
26. P. Meakin, *Phys. Rep.* **235**, 189 (1993).
27. H. van Kranenburg and C. Lodder, *Mat. Sci. Eng.* **R11**, 295 (1994).
28. K. Robbie, J. C. Sit, M. J. Brett, *J. Vac. Sci. Technol. B* **16**, 1115 (1998).
29. Q. Zhang and V. Buch, *J. Chem. Phys.* **92**, 5004 (1990).

30. H. Patashnick, G. Rupprecht, D. W. Schuerman, *Nature* **250**, 313 (1974).
31. R. S. Smith, C. Huang, E. K. L. Wong, B. K. Kay, *Phys. Rev. Lett.* **79**, 909 (1997).
32. J. Klinger, *Science* **209**, 271 (1980).
33. Pacific Northwest National Laboratory is operated for the U.S. Department of Energy by Battelle under contract DE-AC06-76RLO 1830. Supported by the U.S. Department of Energy Office of Basic Energy Sciences, Chemical Sciences Division.

9 October 1998; accepted 27 January 1999

## Semimajor Axis Mobility of Asteroidal Fragments

Paolo Farinella<sup>1\*</sup> and David Vokrouhlický<sup>2</sup>

The semimajor axes of asteroids up to about 20 kilometers in diameter drift as a result of the Yarkovsky effect, a subtle nongravitational mechanism related to radiation pressure recoil on spinning objects that orbit the sun. Over the collisional lifetimes of these objects (typically, 10 to 1000 million years), orbital semimajor axes can be moved by a few hundredths of an astronomical unit for bodies between 1 and 10 kilometers in mean radius. This has implications for the delivery of multikilometer near-Earth asteroids, because the Yarkovsky drift drives many small main-belt asteroids into the resonances that transport them to the Mars-crossing state and eventually to near-Earth space. Recent work has shown that, without such a drift, the Mars-crossing population would be depleted over about 100 million years, a time scale much smaller than the age of the solar system. Moreover, the Yarkovsky semimajor axis mobility may spread in an observable way the tight semimajor axis clustering of small asteroids produced as a consequence of disruptive collisions.

Since their discovery two centuries ago, asteroids have been considered useful “test particles” for celestial mechanics. This is because asteroids are small enough ( $\leq 10^3$  km in diameter) to have negligible gravitational influences on the sun and the planets, while also large enough that gravitation is by far the most important force affecting their orbital motion. Nongravitational forces, arising from interactions with interplanetary dust particles and solar radiation, have been thought to perturb only the orbits of small objects (1, 2), with diameters less than  $\sim 10$  m. Two additional forces—tidal forces in planet-satellite systems and recoil forces due to gas jets from comets—are not relevant for asteroids.

Because of the dominance of gravitational perturbations by the planets, asteroidal orbits undergo long-term ( $\approx 10^4$  years) changes in their inclinations ( $i$ ) and eccentricities ( $e$ ) (3). In most cases, their semimajor axes ( $a$ ) undergo small, short-term periodic perturbations caused by the planets. The asteroids’ semimajor axes have been altered only in the so-called Kirkwood gaps in the main asteroid belt, at semi-

major axes corresponding to strong orbital resonances with Jupiter, and near some other secular resonances with the outer planets. Resonant planetary perturbations have caused the asteroid population to be depleted by large eccentricity jumps leading to encounters or collisions with the planets and the sun. No other dynamical mechanism is thought to have reshaped the basic structure of the distribution of asteroidal semimajor axes since the formation of the solar system. Even disruptive collisions, which may impart to fragments relative speeds of  $\sim 100$  m/s, create families of asteroids whose orbits remain tightly clustered in orbital element space (4, 5).

However, the Yarkovsky effect—a radiation pressure recoil force that acts on anisotropically emitting spinning bodies heated by sunlight to different temperatures in different parts of their surfaces (2, 6)—represents an additional force that may perturb the orbits of small asteroids (sizes up to  $\sim 20$  km in diameter). The original diurnal effect, discovered by the Russian engineer I. O. Yarkovsky about a century ago, is a change in orbital elements, including the semimajor axis, of a rotating asteroidal body as a result of the diurnal changes in its surface temperature distribution. Because the “afternoon” temperature tends to be higher than in the “morning” quadrant, the thermal radiation produces a nonradial recoil force on the body.

<sup>1</sup>Dipartimento di Astronomia, Università di Trieste, Via Tiepolo 11, I-34131 Trieste, Italy. <sup>2</sup>Institute of Astronomy, Charles University, V Holešovickách 2, CZ-18000 Prague 8, Czech Republic.

\*To whom correspondence should be addressed.

More recently, after related work on laser-tracked artificial satellites (7), a “seasonal” variant of the Yarkovsky effect was proposed (8) to be effective for bodies ~10 to 100 m in diameter for transporting them from their source regions in the main asteroid belt (or from Mars) to Earth’s vicinity. This effect is attributable to a component of the force associated with thermal reradiation acting along the polar axis for asteroids with nonzero obliquity. It arises because the hemisphere experiencing “autumn” is hotter (and radiates more thermal energy) than the hemisphere experiencing “spring.”

The diurnal and seasonal Yarkovsky effects act together but depend in different ways on the thermal and rotational properties of the involved bodies, as well as on their sizes. Moreover, for objects undergoing impacts frequently enough to change their polar axes in a random fashion, the seasonal effect causes a variable

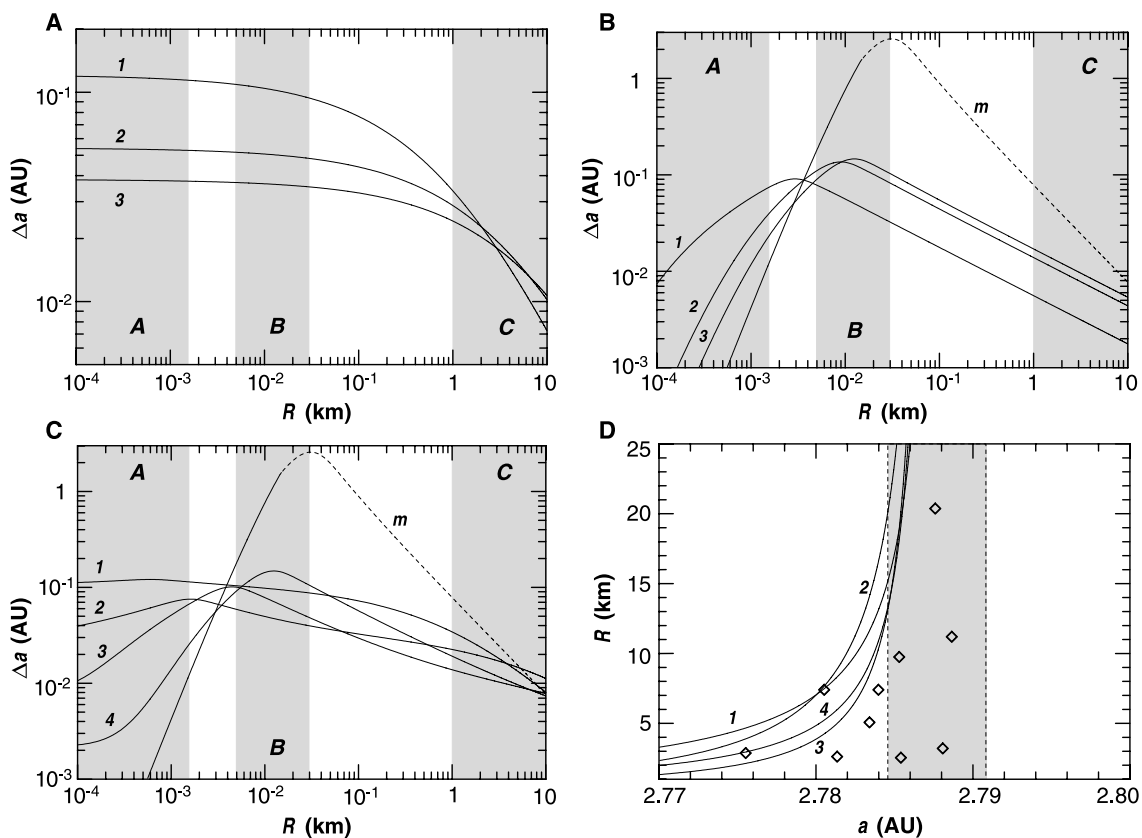
drag-like orbit decay, whereas the diurnal effect results in a kind of random-walk semimajor axis evolution. We proposed that the Yarkovsky-driven semimajor axis drift is important for delivering collisionally generated asteroid fragments to the resonant zones of the inner part of the main belt, from which most meteorites are believed to come (9, 10).

Using recent thermal models for spherical bodies (11), we have calculated how far in semimajor axis the Yarkovsky-driven orbital evolution process typically takes asteroidal fragments of different sizes (up to several tens of kilometers in diameter) over their collisional lifetimes [up to about 1000 million years (My)] (12). For every radius  $R$  and set of material properties [density  $\rho$ , assumed to be 3500 kg/m<sup>3</sup> for silicate-rich bodies (stones) and 8000 kg/m<sup>3</sup> for metal-rich bodies; specific heat  $C$ , 680 J/(kg·K) for stones and 500 J/(kg·K) for metals; and thermal conductivity  $k$ ], we have

considered 10<sup>6</sup> particles with spin periods  $P = 5 \times (R/1 \text{ m}) \text{ s}$  (13) and starting at a semimajor axis  $a = 2.25 \text{ AU}$ . Then we evolved the semimajor axes under both variants of the Yarkovsky effect, reorienting at random the spin axes of the particles to mimic the effects of a sequence of collisions (14). The semimajor axis evolution was followed over the collisional lifetime of each particle, assumed to be given by  $\tau_{\text{dis}} = 16.8 \times (R/1 \text{ m})^{1/2} \text{ My}$  (for stones; for metal-rich bodies we assumed a lifetime about two orders of magnitude longer, up to the age of the solar system). Within a factor 2 of uncertainty, these collisional lifetimes are in agreement with the observed cosmic-ray exposure ages of stony and iron meteorites (15) and the estimated collisional lifetimes of multikilometer main-belt asteroids (12). The average semimajor axis displacement  $\Delta a$  was computed for each simulation.

We have found that for values of  $k$  typical

**Fig. 1.** (A) Average semimajor axis displacement  $\Delta a$  caused by the diurnal Yarkovsky effect within the collisional lifetime  $\tau_{\text{dis}}$  for asteroid fragments of different radii  $R$ . We used three different values for the surface thermal conductivity: (1)  $k = 0.0015 \text{ W/(m·K)}$ , (2)  $k = 0.0075 \text{ W/(m·K)}$ , and (3)  $k = 0.015 \text{ W/(m·K)}$ . The shaded areas correspond to three astronomically important classes of bodies: size range A, pre-atmospheric meteorite parent bodies ( $R = 0.1$  to 1.5 m); size range B, Tunguska-like small NEAs ( $R = 5$  to 30 m); and size range C, the largest existing NEAs ( $R = 1$  to 10 km). We have verified that plausible changes in specific heat, density, and the starting semimajor axis modify these results by less than a factor of 2. (B) The same as (A) but for the seasonal version of the Yarkovsky effect. Higher thermal conductivities of the surface material are assumed here: (1)  $k = 0.1 \text{ W/(m·K)}$ , (2)  $k = 1 \text{ W/(m·K)}$ , and (3)  $k = 2 \text{ W/(m·K)}$ . The  $m$  curve [ $k = 40 \text{ W/(m·K)}$ ] corresponds to metal-rich fragments, whose estimated lifetime is  $>4500 \text{ My}$  for  $R > 15 \text{ m}$  (for larger bodies, corresponding to the dashed part of the curve, we used  $\tau_{\text{dis}} = 4500 \text{ My}$  in our calculations for this case). The maximum  $\Delta a$  mobility for the seasonal effect occurs in size range B, as recently pointed out by Rubincam (8, 11). (C) A composite of the results shown in (A) and (B), with the diurnal and seasonal components of the Yarkovsky effect assumed to act together. Both low- and high-conductivity surfaces are considered here: (1)  $k = 0.002 \text{ W/(m·K)}$ , (2)  $k = 0.02 \text{ W/(m·K)}$ , (3)  $k = 0.2 \text{ W/(m·K)}$ , (4)  $k = 2 \text{ W/(m·K)}$ , and ( $m$  curve)  $k = 40 \text{ W/(m·K)}$ . The low- $k$  cases are dominated by the diurnal effect, whereas for high- $k$  cases the seasonal effect is more important. Note that  $\Delta a$  depends sensitively on the selected value of  $k$  in the A and



B size ranges, but much less so in range C. (D) Proper semimajor axis  $a$  versus radius  $R$  for the known members of the Astrid family ( $\diamond$ ). Note the larger semimajor axis dispersion of the smaller family members. To show that this dispersion is consistent with Yarkovsky mobility, we have assumed that the family was generated 1000 My ago with a small velocity dispersion (10 m/s, comparable to the escape velocity of the largest members; this dispersion corresponds to the shaded strip between the dashed lines). We then plotted the expected Yarkovsky  $\Delta a$  with respect to the largest family member as a function of  $R$ , for different values of the thermal conductivity  $k$ : (1)  $k = 0.002 \text{ W/(m·K)}$ , (2)  $k = 0.02 \text{ W/(m·K)}$ , (3)  $k = 0.2 \text{ W/(m·K)}$ , and (4)  $k = 2 \text{ W/(m·K)}$ . The fact that the smaller family members are preferentially located at smaller semimajor axes suggests an important contribution of the Yarkovsky seasonal effect, corresponding to the higher conductivity cases.

of regolith-free solid rocks, including chondritic meteorites [ $\sim 0.1$  to  $2$  W/(m $\cdot$ K) (16)], and for higher values of  $k$  typical of metal-rich fragments [ $\sim 40$  W/(m $\cdot$ K)], the seasonal effect is in general the dominant one (Fig. 1, A to C). On the other hand, the diurnal effect is more important for values of  $k$  typical of regoliths or particulate stony materials [0.0015 to 0.1 W/(m $\cdot$ K) (17)]. For real asteroid fragments,  $k$  may depend on size, because larger bodies are more likely to retain surface regoliths.

Our simulations considered a range of object sizes, including (i)  $R = 0.1$  to 1.5 m, that is, the typical sizes of meteorites before they enter Earth's atmosphere; (ii)  $R = 5$  to 30 m, corresponding to Tunguska-sized asteroid fragments recently found to be overabundant in near-Earth space (18); and (iii)  $R = 1$  to 10 km, the size range of large near-Earth asteroids (NEAs) capable of causing catastrophic damage if they hit Earth. For the first two size ranges, the Yarkovsky mobility in the asteroid belt appears to be a sensitive function of  $k$ , whereas in the NEA range we get  $\Delta a$  values of 0.008 to 0.03 AU, independent of the value of  $k$ . The direction of this semimajor axis drift depends on the dominant Yarkovsky effect: A systematic inward motion would result when the seasonal effect is stronger, whereas a random walk in either direction would be associated with a dominant diurnal effect.

Our simulations of the subkilometer-size bodies confirm earlier findings on the potential importance of the Yarkovsky effects to deliver the meter-sized pre-atmospheric precursors of meteorites and the small (10 to 100 m in diameter) NEAs from stable main-belt orbits to the main resonances that work as transport routes to near-Earth space (8–11). However, we believe that our model is too simplified to determine detailed quantitative results on the delivery of these small bodies. While they drift in the belt or evolve in resonant orbits, they undergo a kind of “collisional cascade,” so that each initial body is transformed into an evolving swarm of multigenerational fragments, and these are the objects that eventually hit Earth. This is confirmed by the fact that many meteorites display “complex” histories of exposure to cosmic rays, consistent with a sequence of breakup events spread over time spans of tens of millions of years [comparable to  $\tau_{\text{dis}}$  as estimated earlier (19)]. On the other hand, this problem is less serious for the size range 1 to 10 km (in radius), where the collisional lifetime in the main belt is on the order of 1000 My.

The fact that multikilometer-size asteroid fragments move by a few hundredths of an astronomical unit in semimajor axis, after their generation in large-scale collisional events, has important implications for the delivery of NEAs to planet-crossing orbits. Recent work (20) has shown that most multikilometer-size NEAs do not come directly through the pow-

erful 3:1 and  $\nu_6$  resonances in the inner asteroid belt, as previously thought, because these resonances throw most bodies starting from them into sun-grazing orbits within a few million years and therefore would require too high a flux to sustain the existing NEA population in a steady state. Rather, multikilometer-size NEAs probably come from the Mars-crossing asteroid population, which in turn is resupplied by a large number of thin, high-order resonances with Mars and Jupiter located in the inner main belt, which cause a slow chaotic diffusion of the eccentricities of the asteroids (21). However, quantitative studies of this process (21, 22) have shown that the current population of multikilometer-size inner-belt asteroids at moderate eccentricities is too small, at least by a factor of 2, to sustain the Mars-crossing population in a steady state in the long term ( $\sim 100$  My and longer). However, this conclusion holds only if asteroid semimajor axes are assumed to be fixed. Yarkovsky-driven semimajor axis mobility may be instrumental in feeding the high-order resonances with a much higher flux of bodies. There are about 100 thin chaotic resonances in the inner main belt (semimajor axes between 2.15 and 2.45 AU), with average spacings and widths of  $3 \times 10^{-3}$  and  $3 \times 10^{-4}$  AU, respectively (22). Therefore, as a result of Yarkovsky mobility, nearly all the small asteroids will encounter a thin resonance during their collisional lifetime. Collisionally imparted velocity changes are not as effective as the Yarkovsky drift in feeding these resonances, because their collective width ( $\sim 0.03$  AU) is small relative to the total semimajor axis range spanned by the inner belt. This means that newly born, collisionally ejected fragments would have only a  $\sim 10\%$  chance of ending up in a resonance.

In quantitative terms, collisional models (23) show that in the inner belt, collisions create about three fragments per million years that are larger than 5 km in diameter (this rate is uncertain by a factor of 2). If all are injected into the Mars-crossing population through the resonances during their collisional lifetimes of  $\sim 1000$  My, the average feeding rate of about 300 per 100 My is just what is needed to compensate for the dynamical loss of about 360 Mars crossers of this size per 100 My obtained by Migliorini and co-workers (21, 22), and three times the feeding rate derived by these authors assuming only gravitational effects. Without the Yarkovsky effect, collisions would inject into the resonances only about 30 new 5-km fragments per 100 My.

Mostly large asteroids (2 to 20 km in diameter) will be lost from the belt and become Mars crossers through this mechanism, because the Yarkovsky drift rate for these bodies is slow enough ( $\sim 10^{-5}$  AU/My) for the thin resonances to be able to pump up the eccentricity by a large amount over the characteristic time scales of a few tens of millions of years for resonant diffusion of the eccentricity. On the other hand,

the flux problem does not exist for the kilometer-size and smaller NEAs, whose populations can be maintained in steady state by the main 3:1 and  $\nu_6$  resonances alone (23, 24). Thus, we suggest that the delivery of large NEAs may be a complex, multistage process, starting from a collisional breakup in the inner belt (possibly forming an asteroid family), followed by slow semimajor axis drift under Yarkovsky effects, then chaotic diffusion of eccentricity in a thin resonance up to Mars-crossing, and eventually injection into an Earth-crossing orbit by a strong resonance. NEAs smaller than  $\sim 1$  km, on the other hand, are likely to skip the thin-resonance stage.

An independent test of the role of the Yarkovsky drift comes from the analysis of the orbital distribution of small main-belt asteroids. Some asteroid families are compact clusters in proper element space, with typical semimajor axis ranges of a few hundredths of an astronomical unit. Unfortunately, because of observational selection effects, only a few such families are known with a large enough number of members having diameters smaller than 20 km. The best case identified in the most recent and comprehensive family search (5) is that of the Astrid family, a very compact cluster of 10 small asteroids located at a semimajor axis of about 2.78 AU. For the Astrid family members, despite the limited number of objects available, the semimajor axis range in the family is larger at smaller sizes, consistent with Yarkovsky mobility (Fig. 1D). We cannot exclude the possibility that a higher (and possibly size-dependent) initial ejection velocity of the family members is also playing a role here.

Another way to test whether the Yarkovsky drift alters real asteroidal orbital elements is to look at the orbits of small ( $\leq 20$  km in diameter) asteroids close to the edges of the Kirkwood gaps associated with the main jovian resonances. Nakamura (25) has observed that near the edges of these gaps there is a gradient of mean asteroid sizes, with more of the smaller bodies closer to the centers of the gaps. The effect is apparent at diameters of  $\sim 10$  km over a semimajor axis range of  $\sim 0.01$  AU. Again, this can be interpreted in terms of a size dependence of fragment speeds following ejection after asteroidal breakup events (26), but an alternative interpretation is that Yarkovsky mobility may gradually bring into the resonances small fragments originally formed “on the brink.” A specific case of this type is possibly 2953 Vysheslavlia, a 15-km-diameter member of the Koronis asteroid family whose semimajor axis is so close to the edge of the 5:2 gap that its orbit will become unstable and fall into the strongly chaotic portion of the resonance within a few tens of millions of years (27). Other small members of the family may be on their way to a similar fate (28).

Finally, the Yarkovsky semimajor axis drift may be important in transporting to the main resonances a large number of bodies around 10 m in radius for which  $\Delta a$  values of  $\sim 0.1$  AU are expected (Fig. 1C), similar to the distances between the main Kirkwood gaps. These fragments may be removed from the main belt population faster than bodies of other sizes, and in turn this may result into longer collisional lifetimes  $\tau_{\text{dis}}$  for the 100-m objects, which would also become more mobile (29). Although a realistic model of the feedback effects between Yarkovsky orbital drift and collisional processing of the asteroid size distribution would be required to assess these effects, we suggest that the Yarkovsky mobility mechanism may provide a plausible explanation for the observed overabundance of bodies 10 to 100 m in diameter in the near-Earth population (18).

References and Notes

1. A. Milani, A. M. Nobili, P. Farinella, *Non-Gravitational Perturbations and Satellite Geodesy* (Hilger, Bristol, UK, 1987).
2. J. A. Burns, P. L. Lamy, S. Soter, *Icarus* **40**, 1 (1979).
3. D. Brouwer and G. M. Clemence, *Methods of Celestial Mechanics* (Academic Press, New York, 1961), chap. 16.
4. C. R. Chapman et al., in *Asteroids II*, R. P. Binzel, T. Gehrels, M. S. Matthews, Eds. (Univ. of Arizona Press, Tucson, AZ, 1989), pp. 386–415.
5. V. Zappalà et al., *Icarus* **116**, 291 (1995).
6. E. J. Öpik, *Proc. R. Irish Acad.* **54**, 165 (1951); V. V. Radzievskii, *Astron. Zh.* **29**, 162 (1952); C. Peterson, *Icarus* **29**, 91 (1976); G. Afonso, R. S. Gomes, M. A. Florczak, *Planet. Space Sci.* **43**, 787 (1995).
7. D. P. Rubincam, *J. Geophys. Res.* **92**, 1287 (1987); P. Farinella and D. Vokrouhlický, *Planet. Space Sci.* **44**, 1551 (1996); V. J. Slabinski, *Celest. Mech. Dyn. Astron.* **66**, 131 (1997).
8. D. P. Rubincam, *J. Geophys. Res.* **100**, 1585 (1995).
9. P. Farinella, D. Vokrouhlický, W. K. Hartmann, *Icarus* **132**, 378 (1998).
10. D. Vokrouhlický and P. Farinella, *Astron. Astrophys.* **335**, 351 (1998); W. K. Hartmann et al., *Meteorit. Planet. Sci.*, in press.
11. For the seasonal effect, see D. P. Rubincam, *J. Geophys. Res.* **103**, 1725 (1998); D. Vokrouhlický and P. Farinella, *Astron. J.* **116**, 2032 (1998); for the diurnal effect, see D. Vokrouhlický, *Astron. Astrophys.* **335**, 1093 (1998).
12. D. R. Davis et al., in (4), pp. 805–826; P. Farinella et al., *Astron. Astrophys.* **257**, 329 (1992); R. Greenberg et al., *Icarus* **107**, 84 (1994); D. R. Davis et al., *ibid.* **120**, 220 (1996).
13. Such a relation is roughly in agreement with the results of laboratory experiments on the catastrophic fragmentation of bodies  $\sim 20$  cm in diameter [I. Gliblin et al., *Icarus* **110**, 203 (1994); *ibid.* **134**, 77 (1998)], with the inferred rotation rate of the Lost City fireball [3.3 s for a diameter of  $\sim 0.5$  m; see Z. Ceplecha, *Astron. Astrophys.* **311**, 329 (1992)], with the  $\sim 10$  min spin rate of the small NEA 1998 KY<sub>26</sub> (several tens of meters across) [P. Pravec and L. Sarounova, *IAU Circ.* **6941**, 2 (1998)], and with the typical spin periods of several hours for small main-belt asteroids [R. P. Binzel et al., in (4), pp. 416–441].
14. At each time step  $\Delta t$  we computed a spin axis reorientation probability  $P = 1 - \exp(-\Delta t / \tau_{\text{rot}})$ , where  $\tau_{\text{rot}} = 15.0 \times (R/1 \text{ m})^{1/2}$  My for stony bodies and  $\tau_{\text{rot}} = 37.5 \times (R/1 \text{ m})^{1/2}$  My for metal-rich bodies. We then used a Monte Carlo procedure to select the particles to be reoriented. The normalizing coefficient of the  $\tau_{\text{rot}}$  formula is in agreement with our assumed relation between spin rate and size, and is about 4.5 times the value adopted in (9). This results in a diurnal Yarkovsky drift about 1.7 times

15. M. W. Caffee et al., in *Meteorites and the Early Solar System*, J. F. Kerridge and M. S. Matthews, Eds. (Univ. of Arizona Press, Tucson, AZ, 1988), pp. 205–245; K. Marti and T. Graf, *Annu. Rev. Earth Planet. Sci.* **20**, 221 (1992). As explained in (9), this relation between  $\tau_{\text{dis}}$  and  $R$  is also consistent with the steady-state size distribution of small asteroid fragments predicted in (30).
16. K. Yomogida and T. Matsui, *J. Geophys. Res.* **88**, 9513 (1983).
17. For the upper layer of the lunar regolith, a typical value of 0.0015 W/(m<sup>2</sup>K) has been reported [M. G. Langseth, S. J. Keihm, J. L. Chute, in *Apollo 17—Preliminary Science Report*, NASA SP-330 (1973)]. Measurements for porous or particulate stony materials have been performed [A. E. Wechsler, P. E. Glaser, A. D. Little, J. A. Fountain, in *Thermal Characteristics of the Moon*, J. W. Lucas, Ed. (MIT Press, Cambridge, MA, 1972), pp. 215–242; see also M. A. Presley and P. R. Christensen, *J. Geophys. Res.* **102**, 6551 (1997)].
18. D. P. Rabinowitz, *Astrophys. J.* **407**, 412 (1993); *Icarus* **111**, 364 (1994); *ibid.* **130**, 287 (1998); P. Farinella and M. Menichella, *Planet. Space Sci.* **46**, 303 (1998).
19. G. W. Wetherill, *Meteoritics* **15**, 386 (1980); G. F. Herzog et al., *Meteorit. Planet. Sci.* **32**, 413 (1997).
20. P. Farinella et al., *Nature* **371**, 314 (1994); F. Migliorini et al., *Meteorit. Planet. Sci.* **32**, 903 (1997); B. J. Gladman et al., *Science* **277**, 197 (1997).

21. F. Migliorini et al., *Science* **281**, 2022 (1998).
22. A. Morbidelli and D. Nesvorný, *Icarus*, in press.
23. M. Menichella et al., *Earth Moon Planets* **72**, 133 (1996).
24. A. Morbidelli and B. J. Gladman, *Meteorit. Planet. Sci.* **33**, 999 (1998).
25. T. Nakamura, in *Seventy-Five Years of Hirayama Asteroid Families*, Y. Kozai, R. P. Binzel, T. Hirayama, Eds. (Astronomical Society of the Pacific, San Francisco, 1994), Conference Series vol. 63, pp. 52–61.
26. Such a relation has been reported [A. M. Nakamura and A. Fujiwara, *Icarus* **92**, 132 (1991); \_\_\_\_\_, T. Kadono, *Planet. Space Sci.* **42**, 1043 (1994)]. On the other hand, recent experimental results [I. Gliblin, *ibid.* **46**, 921 (1998)] show that the fragment size-velocity correlation is probably weak and dependent on the experimental setup.
27. A. Milani and P. Farinella, *Icarus* **115**, 209 (1995).
28. Z. Knežević, A. Milani, P. Farinella, *Planet. Space Sci.* **45**, 1581 (1998).
29. In Fig. 1, A to C, we did not take into account these feedback effects, and just assumed  $\tau_{\text{dis}} \propto R^{1/2}$ , consistent with the equilibrium size distribution predicted in (30) for scale-independent collisional systems. However, if the "Yarkovsky sink" is effective for objects  $\sim 10$  m in radius, this may introduce a lower-cutoff effect in the size distribution, resulting in a wave-like pattern superimposed on the Dohnanyi power-law size distribution [see A. Campo Bagatin et al., *Planet. Space Sci.* **42**, 1079 (1994)].
30. J. W. Dohnanyi, *J. Geophys. Res.* **74**, 2531 (1969).

16 September 1998; accepted 25 January 1999

# Quartzlike Carbon Dioxide: An Optically Nonlinear Extended Solid at High Pressures and Temperatures

V. Iota, C. S. Yoo,\* H. Cynn

An extended-solid phase, carbon dioxide phase V (CO<sub>2</sub>-V), was synthesized in a diamond anvil cell by laser heating the molecular orthorhombic phase, carbon dioxide phase III, above 40 gigapascals and 1800 kelvin. This new material can be quenched to ambient temperature above 1 gigapascal. The vibration spectrum of CO<sub>2</sub>-V is similar to that of the quartz polymorph of silicon dioxide, indicating that it is an extended covalent solid with carbon-oxygen single bonds. This material is also optically nonlinear, generating the second harmonic of a neodymium-yttrium-lithium-fluoride laser at a wavelength of 527 nanometers with a conversion efficiency that is near 0.1 percent.

High pressure alters the nature of chemical bonds, electronic and crystal structures, and thermal and mechanical properties of solids. It has been suggested that simple molecular solids may transform into a polymeric phase before they become metals at high pressure (1). Theoretical models and experimental data support this hypothesis, including polymeric forms of N<sub>2</sub> (1), CO (2), diamond (3), β-C<sub>3</sub>N<sub>4</sub> (4), and symmetric H<sub>2</sub>O (5). Furthermore, these pressure-induced changes often occur in systematic

ways, providing new routes for designing and synthesizing novel materials with advanced optical and mechanical properties. The structures of the N<sub>2</sub> polymer, diamond, and β-C<sub>3</sub>N<sub>4</sub> at high pressures, for example, can be viewed as being similar to the assemblages of heavier elements in each periodic group (P, Si, and β-Si<sub>3</sub>N<sub>4</sub>, respectively) at low pressures.

Carbon dioxide is one of the most abundant volatile materials on Earth. Also, CO<sub>2</sub> crystals (dry ice) are widely used for cooling, and CO<sub>2</sub> is found as clathrates on Mars and other planets (6). However, the properties of CO<sub>2</sub> at high pressures are not well understood. Four polymorphs have been suggested for CO<sub>2</sub>, but the structures and stability of

Lawrence Livermore National Laboratory, University of California, Livermore, CA 94551, USA.

\*To whom correspondence should be addressed. E-mail: yoo1@llnl.gov